Histomorphometry and Bone Mechanical Property Evolution Around Different Implant Systems at Early Healing Stages. An Experimental Study in Dogs

Synopsis

Authors:

Ryo Jimbo[1], Rodolfo Anchieta[2], Marta Baldassarri[3], Rodrigo Granato[4], Charles Marin[5], Hellen S. Teixeira[6], Nick Tovar[7], Stefan Vandeweghe[8], Malvin N. Janal[9], and Paulo G. Coelho[10]

1. Associate Professor, Department of Prosthodontics, Faculty of Odontology, Malmö University, Malmö, Sweden
2. Researcher, Department of Biomaterials and Biomimetics, New York University College of Dentistry, New York USA, Private Practice, Paris, France
3. Researcher, Department of Biomaterials and Biomimetics, New York University College of Dentistry, New York USA
4. Lecturer, Department of Dentistry, Universidade Federal de Santa Catarina, Florianopolis, Brazil
5. Lecturer, Department of Dentistry, Universidade Federal de Santa Catarina, Florianopolis, Brazil
6. Researcher, Department of Biomaterials and Biomimetics, New York University College of Dentistry, New York USA
7. Adjunct Professor, Department of Biomaterials and Biomimetics, New York University College of Dentistry, New York USA
8. Assistant Professor, Department of Periodontology and Oral Implantology, Dental School, Faculty of Medicine and Health sciences, University of Ghent, Belgium
9. Senior Research Scientist, Department of Epidemiology, New York University College of Dentistry, New York USA
10. Assistant Professor of Biomaterials and Biomimetics & Director for Research, Department of Periodontology and Implant Dentistry, New York University College of Dentistry, New York USA Correspondence to; Ryo Jimbo, Department of Prostho dontics, Faculty of Odontology, Malmö University, 205 06 Malmö, Sweden

Objective:

The aim of this in vivo animal study is to evaluate the osteoconductivity of 5 different commercially available implants histomorphometrically, and further to evaluate the bone nanomechanical properties using the nanoindentation technique.

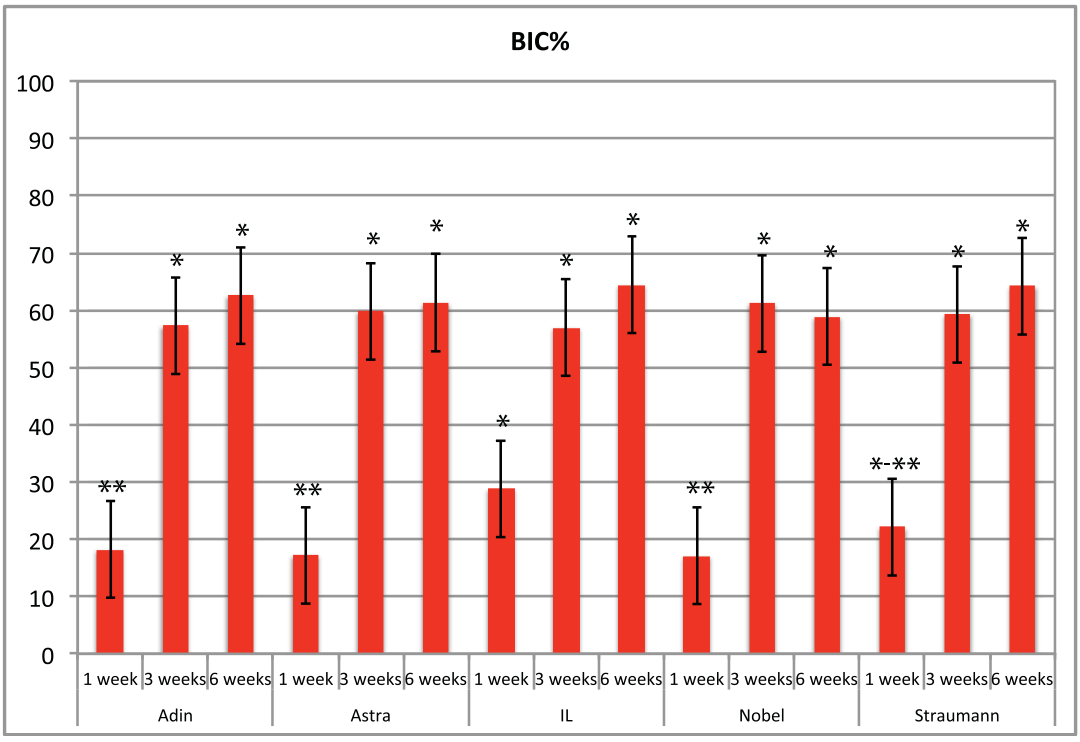

Figure 1: BIC as a function of implant system and time in vivo. Note that the number of asterisks represents statistically homogeneous groups for each individual time in vivo.

Note: Study report is currently under publication. Complete version is available upon request.

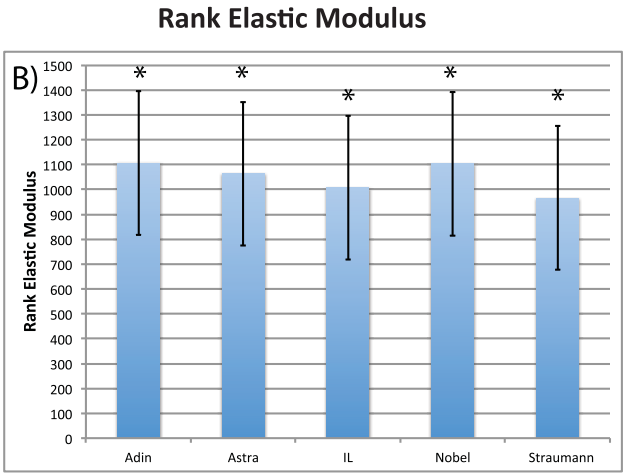

Figure 2: Rank elastic modulus as a function of (b) implant system. Note that the number of asterisks depict statistically homogeneous groups.

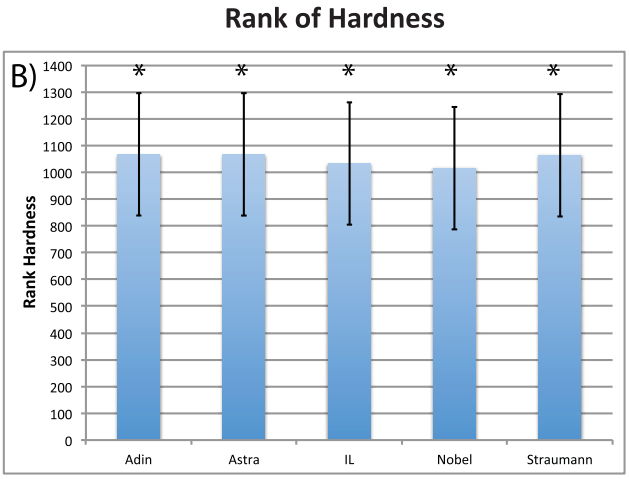

Figure 3: Rank hardness as a function of (b) implant system. Note that the number of asterisks depict statistically homogeneous groups.

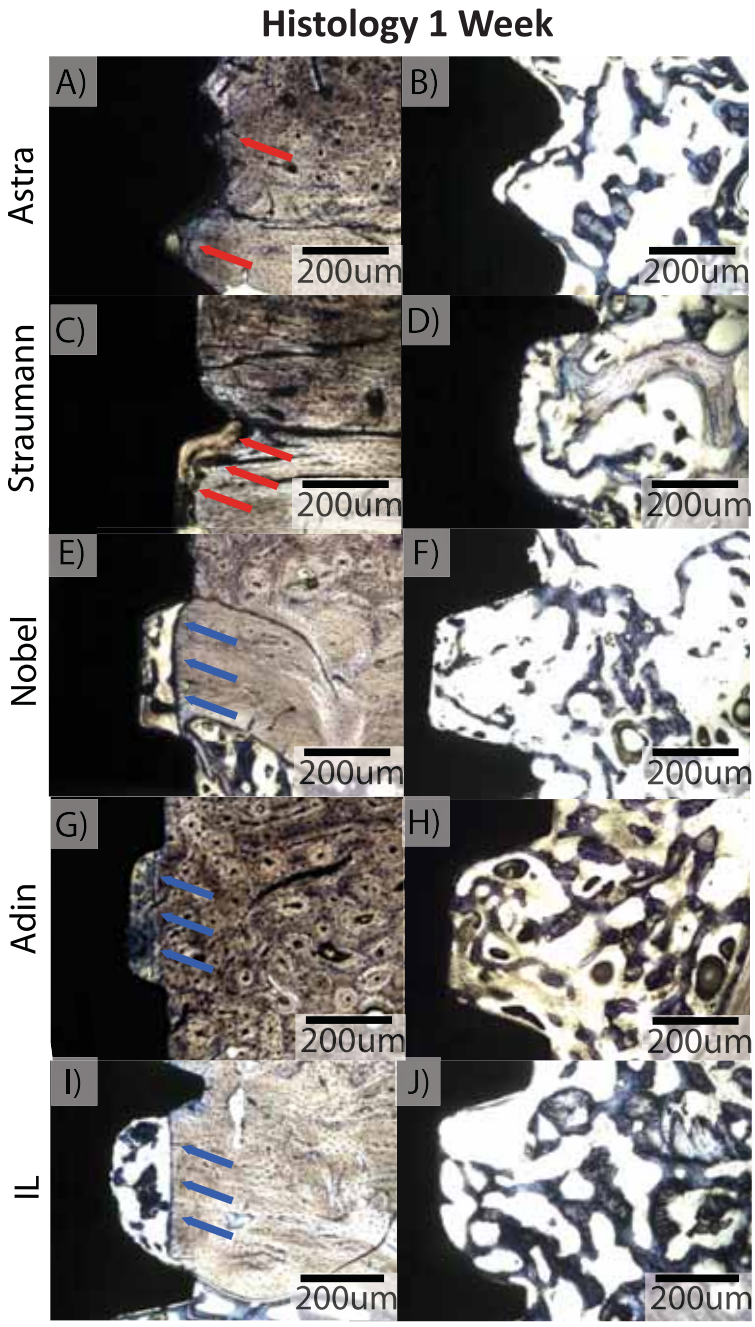

Figure 2: One week in vivo optical micrographs of Astra Osseospeed at (a) cortical region and (b) trabecular regions, Straumann SLA at (c) cortical region and (d) trabecular regions, Nobel Active at (e) cortical region and (f) trabecular regions, Adin Osseofix at (g) cortical region and (h) trabecular regions, and IL Ossean at (i) cortical region and (j) trabecular regions. In regions of cortical bone, initial interface remodelling was observed at the regions where direct engagement between implant and bone existed at the cortical immediately after placement (Astra Osseospeed implant microthread regions and the Straumann SLA cervical third, red arrows in a and c). For the other three systems, the interplay between the implant bulk design and drilling dimensions allowed for empty spaces (healing chambers, denoted by blue arrows in e, g, and i) of different dimensions bounded by the implant surface and cortical bone, which at 1 week presented initial woven bone formation . In regions of trabecular bone, initial formation of woven bone was observed in direct contact or in proximity of all implant surfaces (b, d, f, h, j).

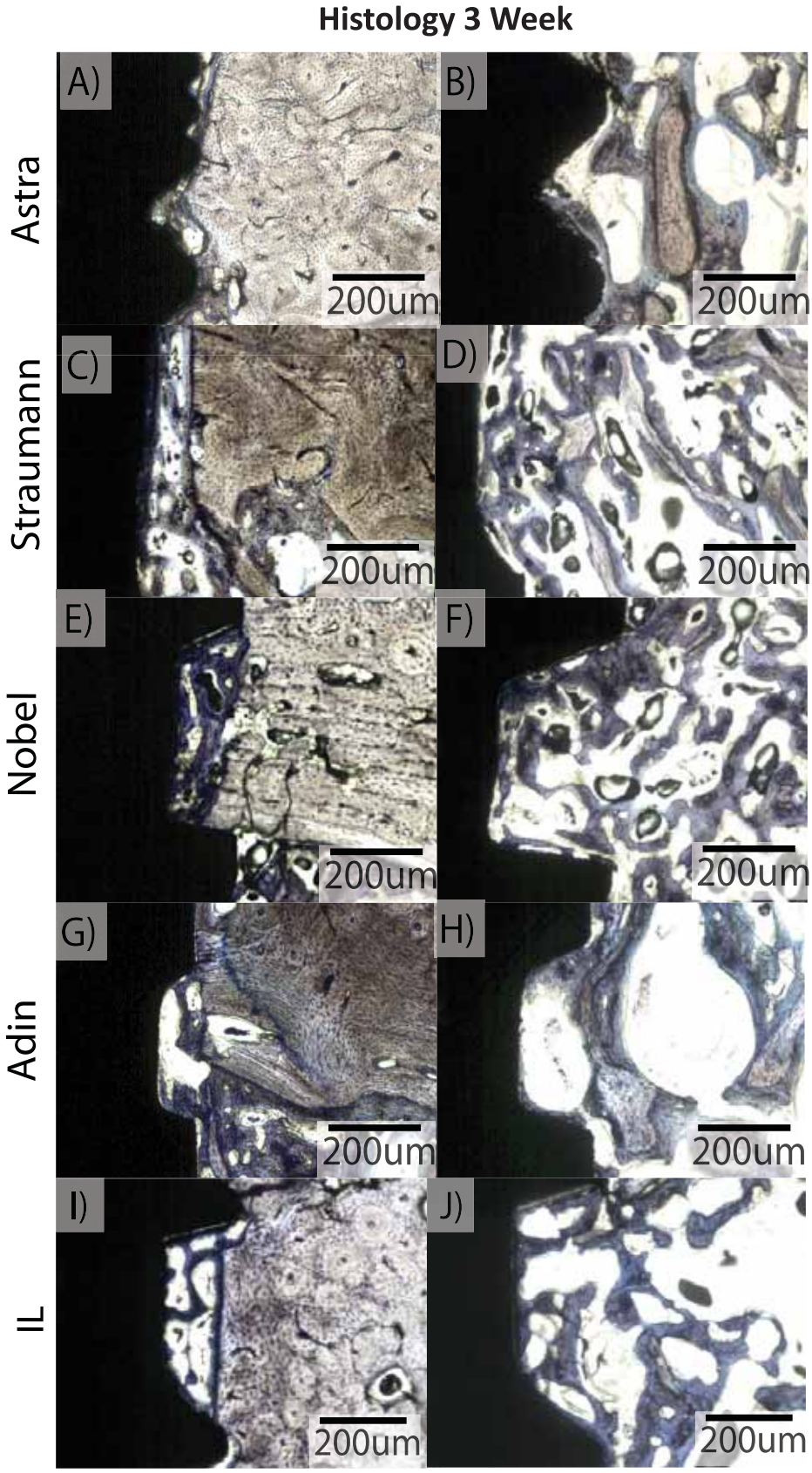

Figure 3: Three weeks in vivo optical micrographs of Astra Osseospeed at (a) cortical region and (b) trabecular regions, Straumann SLA at (c) cortical region and (d) trabecular regions, Nobel Active at (e) cortical region and (f) trabecular regions, Adin Osseofix at (g) cortical region and (h) trabecular regions, and IL Ossean at (i) cortical region and (j) trabecular regions. In regions of cortical bone where primary engagement occurred immediately after implant placement, interfacial remodelling resulted in newly formed bone filling the gap between cortical bone and implant surface (a and c). On the other hand, implant system that allowed the formation of healing chambers showed higher degree of interaction between bone and implant surface (e, g, and i). In regions of trabecular bone, formation of woven bone progressed relative to the 1 week time point either in direct contact or in proximity of all implant surfaces (b, d, f, h, j). In these regions, initial woven bone remodelling sites were seldom observed.

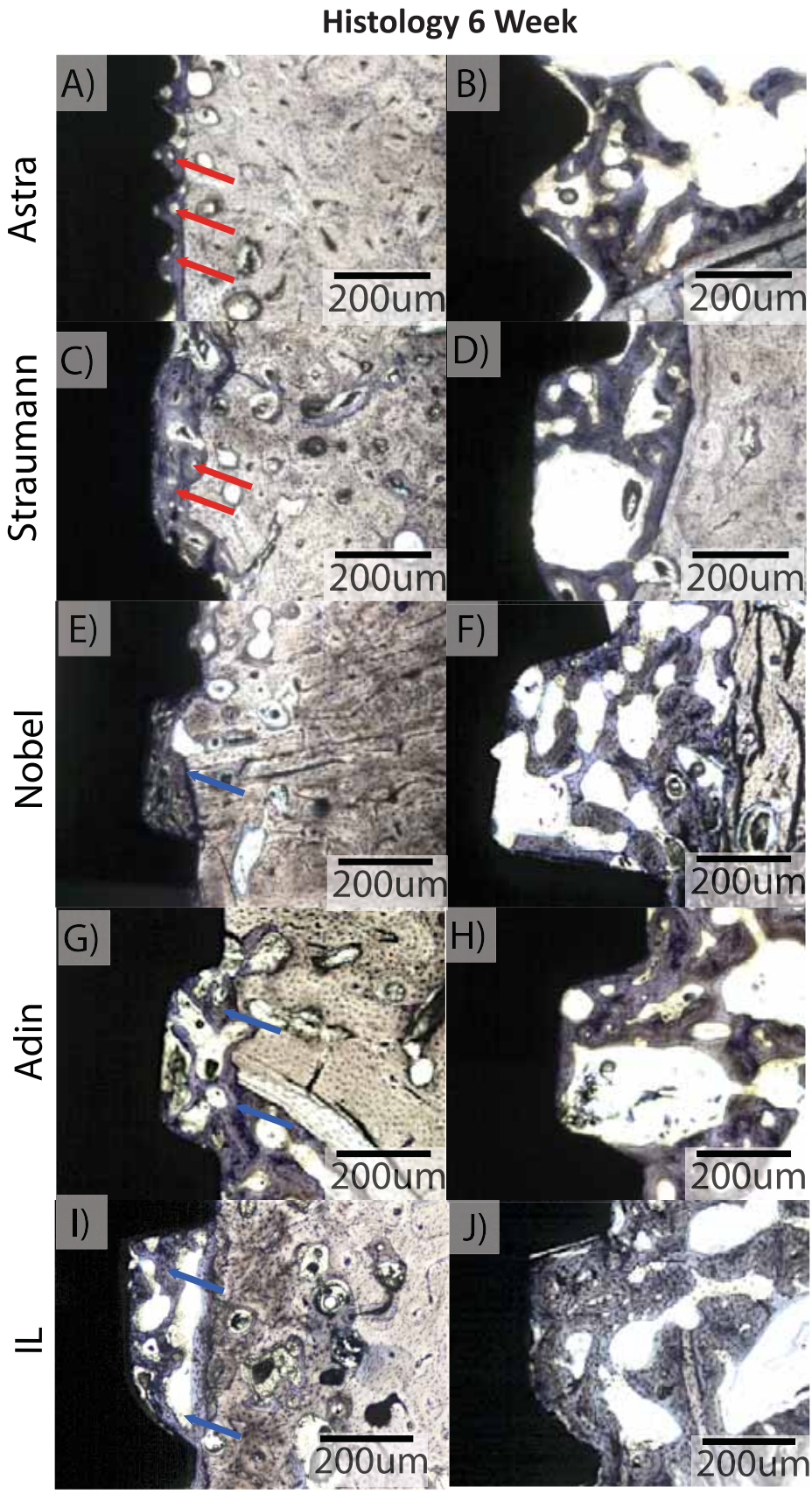

Figure 4: Six weeks in vivo optical micrographs of Astra Osseospeed at (a) cortical region and (b) trabecular regions, Straumann SLA at (c) cortical region and (d) trabecular regions, Nobel Active at (e) cortical region and (f) trabecular regions, Adin Osseofix at (g) cortical region and (h) trabecular regions, and IL Ossean at (i) cortical region and (j) trabecular regions. in regions of cortical bone where primary engagement occurred immediately after implant placement, bone remodeling sites were observed on the woven bone filling the gap between cortical bone and implant surface (red arrows in a and c). For the implant systems that allowed the formation of healing chambers, initial replacement of woven bone by lamellar bone was observed (blue arrows on e, g, and i). In regions of trabecular bone, initial replacement of woven bone by lamellar bone was observed irrespective of implant group (b, d, f, h, j). In these regions, multiple bone remodelling sites were observed.